

# Performance of apparent diffusion coefficient values and ratios for the prediction of prostate cancer aggressiveness across different MRI acquisition settings

Ercan Karaarslan  
Aylin Altan Kus   
Deniz Alis   
Umut Can Karaarslan   
Yesim Saglican  
Omer Burak Argun   
Ali Riza Kural 

## PURPOSE

In this study, we assessed the performance of apparent diffusion coefficient (ADC) and diffusion-weighted imaging (DWI) metrics and their ratios across different magnetic resonance imaging (MRI) acquisition settings, with or without an endorectal coil (ERC), for the evaluation of prostate cancer (PCa) aggressiveness using whole-mount specimens as a reference.

## METHODS

We retrospectively reviewed the data of pCa patients with a Gleason score (GS) of 3 + 4 or higher who underwent prostate MRI using a 3T unit at our institution. They were divided into two groups based on the use of ERC for MRI acquisition, and patients who underwent prostate MRI with an ERC constituted the ERC (n = 55) data set, while the remaining patients accounted for the non-ERC data set (n = 41). DWI was performed with b-values of 50, 500, 1000, and 1400 s/mm<sup>2</sup>, and ADC maps were automatically calculated. Additionally, computed DWI (cDWI) was performed with a b-value of 2000 s/mm<sup>2</sup>. Six ADC and two cDWI parameters were evaluated. In the ERC data set, receiver operating characteristic curves were plotted for each metric to determine the best cutoff threshold values for differentiating GS 3 + 4 PCa from that with a higher GS. The performance of these cutoff values was assessed in non-ERC data set. The diagnostic accuracies and area under the curves (AUCs) of the metrics were compared using Fisher exact test and De Long method, respectively.

## RESULTS

Among all metrics, the mean ADC ratio of the tumor to normal prostate ( $ADC_{\text{mean-ratio}}$ ) yielded the highest AUC, 0.84, for differentiating GS 3 + 4 PCa from that with a higher GS. The best threshold cutoff values of  $ADC_{\text{mean-ratio}} (\leq 0.51)$  for discriminating GS 3 + 4 PCa from that with a higher GS correctly classified 48 of 55 patients with an accuracy of 87.27%. However, there was no significant difference between the metrics in terms of accuracy and AUC ( $P = .163$  and  $P = .214$ ). Similarly, in the non-ERC data set, the  $ADC_{\text{mean-ratio}}$  provided the highest diagnostic accuracy (82.92%) by classifying 34 of 41 patients. However, Fisher exact test yielded no significant difference between DWI and ADC metrics in terms of diagnostic accuracy in non-ERC data ( $P = .561$ ).

## CONCLUSION

The mean ADC ratio of the tumor to normal prostate showed the highest accuracy and AUC in differentiating GS 3 + 4 PCa and PCa with a higher GS across different MRI acquisition settings; however, the performance of different ADC and DWI metrics did not differ significantly.

Improvements in state-of-the-art magnetic resonance imaging (MRI) have resulted in an exponential increase in the employment of this technique for prostate cancer (PCa). Diffusion-weighted imaging (DWI) with apparent diffusion coefficient (ADC) maps is the key component of the current multiparametric MRI (mpMRI) protocol.<sup>1</sup> Over the years, clinical applications of mpMRI have evolved from PCa detection and staging to noninvasive characterization of tumor in which ADC metrics play a necessary role.<sup>2–4</sup> ADC metrics, as a preoperative noninvasive measure of the Gleason score (GS), which reflects PCa aggressiveness, have gained considerable research attention, since the preoperative GS obtained with an ultrasound-guided needle core biopsy is subject to sampling errors.<sup>5</sup> Furthermore, upgrading or downgrading of GS occurs in a non-negligible proportion of

From the Departments of Radiology (E.K. ✉ ercan.karaarslan@acibadem.edu.tr, A.A.K., D.A.), (U.C.K.), Pathology (Y.S.), and Urology (O.B.A., A.R.K.), Acibadem Mehmet Ali Aydinlar University, School of Medicine, Istanbul, Turkey.

Received 2 September 2020; revision requested 25 September 2020; last revision received 16 November 2020; accepted 29 November 2020.

DOI: 10.5152/dir.2022.20732

You may cite this article as: Karaarslan E, Kus AA, Alis D, Karaarslan UC, Saglican Y, Argun OB, Performance of apparent diffusion coefficient values and ratios for the prediction of prostate cancer aggressiveness across different MRI acquisition settings. *Diagn Interv Radiol.* 2022; 28(1):12–20.

the subjects when verified by a whole-mount histopathological analysis after prostatectomy.<sup>5</sup>

Previous studies introduced several absolute ADC metrics as surrogate-markers in predicting PCa aggressiveness.<sup>2-4</sup> In following studies, researchers pointed out the variability of absolute ADC metrics caused by technical or patient-related factors and advocated that tumor-to-prostate ADC ratios are more reliable and better parameters,<sup>6-9</sup> yet several studies have failed to demonstrate any advantage of using ADC ratios.<sup>10-12</sup> Use of the whole prostate gland as a denominator for calculating ADC ratios, instead of healthy prostatic tissue, and the assessment of the signal intensity (SI) of PCa on DWI have been evaluated in this context with variable success.<sup>13-15</sup> Although ongoing discussions regarding the performance of the mentioned metrics are strongly related to the technical factors, only few studies have investigated the success of these metrics across different MRI acquisition settings.<sup>16-18</sup>

In this study, we investigated the optimum cutoff threshold values of several quantitative ADC and DWI metrics in differentiating GS 3 + 4 PCa patients from those with higher GS using whole-mount specimens as the reference method in patients who underwent mpMRI on a 3T unit with an endorectal coil (ERC). The determined cutoff threshold values were applied to another subset of patients with PCa who underwent mpMRI on the same scanner without an ERC to test whether the ADC- and DWI-derived

ratios would show better performance than their absolute counterparts.

## Methods

The local ethics committee approved this retrospective study carried out between January 2016 and December 2018 and waived the need for informed consent because of the retrospective evaluation of anonymized medical data (Approval ID: 20201222). We retrospectively reviewed all consecutive patient data who underwent radical prostatectomy for PCa at our institution to identify patients with whole-mount pathology specimens yielding GS 3 + 4 or higher GS PCa.<sup>19</sup> The inclusion criteria were as follows: (1) prostate mpMRI obtained on a 3T unit within 6 months before the operation and at least 6 weeks after the prostate biopsy to mitigate biopsy-related artifacts, (2) available serum prostate-specific antigen (PSA) levels at the time of prostate mpMRI, (3) available whole-mount specimen, and (4) index lesion with a volume >0.5 mL in a whole-mount specimen. The exclusion criteria were as follows: (1) patients who received prior androgen deprivation therapy, radiotherapy, or transurethral resection of the prostate; (2) patients with prostate

mpMRI scan with incomplete sequences or inadequate image quality; and (3) index lesions with a diameter <5 mm seen on prostate mpMRI. Figure 1 illustrates the patient selection procedure of the study.

The study sample was divided into two subgroups: the ERC and the non-ERC data sets. The ERC data set comprised the patients who underwent mpMRI with an ERC and was used to determine the optimum cutoff threshold values of quantitative ADC and DWI parameters for differentiating GS 3 + 4 PCa patients from those with a higher GS. The non-ERC data set comprised the patients in whom mpMRI was performed without an ERC and was used to evaluate the diagnostic performance of the pre-determined cutoff threshold values in assessing PCa aggressiveness.

All patients underwent prostate mpMRI on a 3.0 Tesla MRI scanner (Skyra, Siemens Medical Systems). Prostate mpMRI was performed with an 18-channel phased-array coil and a liquid perfluorocarbon-filled ERC (Medrad, Bayer) in the ERC data set. Prostate mpMRI was performed with the same coil in the non-ERC data set. For all examinations, butylscopolamine bromide (Buscopan, Boehringer Ingelheim) was

### Main points

- A threshold value of the mean ADC ratio of the tumor to normal prostate ( $ADC_{\text{mean-ratio}}$ ) of  $\leq 0.51$ , which was determined in patients who underwent prostate MRI with an ERC, could accurately differ GS 3 + 4 PCa from that with a higher GS in another subset of patients who underwent prostate MRI without an ERC.
- $ADC_{\text{mean-ratio}}$  consistently showed the highest diagnostic accuracy in differentiating GS 3 + 4 PCa from that with a higher GS across different data sets in which prostate mpMRI was performed with and without an ERC, though without any significant difference.
- The  $ADC_{\text{mean-ratio}}$  might be of clinical value as a reliable and precise metric in assessing PCa aggressiveness, yet further work is warranted to precisely reveal whether it outperforms other ADC and DWI metrics.

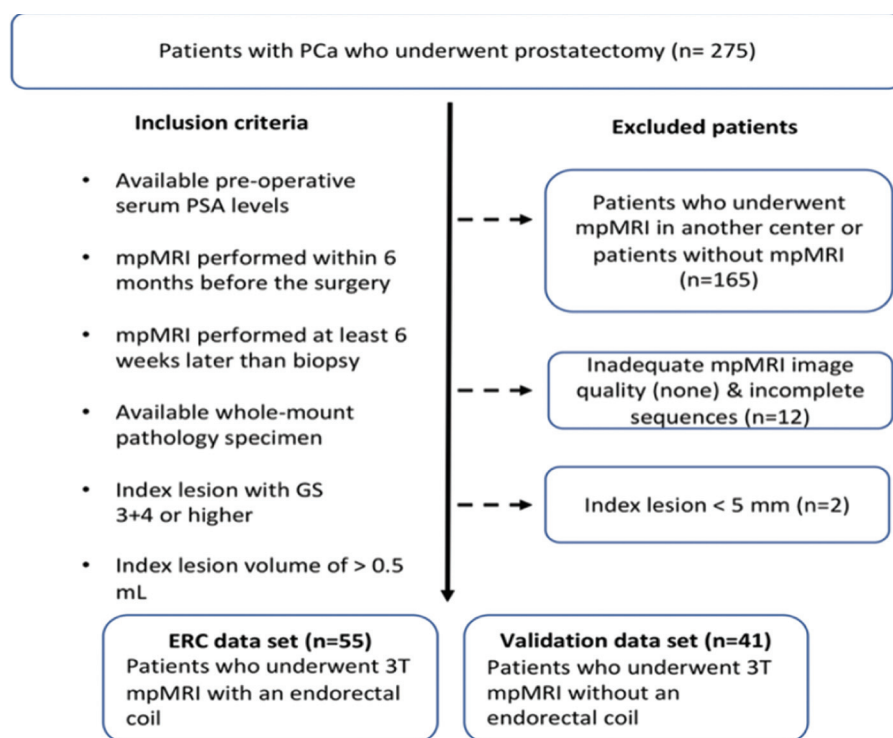


**Figure 1.** The flowchart of patient selection. PCa, prostate cancer; PSA, prostate serum antigen; mpMRI, multiparametric magnetic resonance imaging; GS, Gleason; ERC, endorectal coil.

injected to reduce bowel movements that might cause motion artifacts. The mpMRI protocol of our institution was tailored by a senior radiologist with over 26 years of prostate MRI interpretation experience considering the recommendations of the PI-RADS committee.<sup>2</sup> The prostate mpMRI protocol (in the order of the first to last technique) consisted of tri-planar T2-weighted imaging, DWI, and dynamic contrast-enhanced (DCE) imaging. DWI was performed using echo-planar imaging in axial planes at different b-values of 50, 500, 1000, and 1400 s/mm<sup>2</sup>. The ADC maps were calculated automatically by the software using all available b-values (Syngo via, Siemens Medical Systems) integrated into the least-square mono-exponential fitting. The formula for calculating the ADC maps was as follows:  $ADC = -\ln(S/S_0)/b$ , where  $S_0$  is the SI of no diffusion gradients and  $b$  is the b-value. After the acquisition, computed DWI (cDWI) was calculated with a b-value of 2000 s/mm<sup>2</sup>.

The detailed parameters regarding the MRI sequences are given in Supplementary Table S1. A genitourinary pathologist with 25 years of experience interpreted all prostatectomy specimens. The specimens were prepared and interpreted according to relevant international guidelines.<sup>20</sup> Macroscopic images of the specimens were digitalized. Subsequently, the pathologist highlighted the areas containing tumor foci and index lesions on the corresponding macroscopic specimen. The index tumor was accepted as the tumor focus with the highest GS. In cases involving the presence of two tumor foci with the same GS, the tumor with the larger size was accepted as the index lesion.<sup>21</sup>

A radiologist with 5 years of prostate mpMRI experience and the genitourinary pathologist mutually evaluated the index lesion on prostate mpMRI, with respect to the histopathological images of the whole-mount specimen to ensure a radio-pathological match. The radiologist was free to assess the radiologic reports of the patients, which were interpreted by a senior radiologist according to PI-RADS version 2. The window level for the assessment was adjusted according to the observer's preferences for each case. The observer drew a free-hand region of interest (ROI) onto the tumor using an ADC map that included the tumor with the largest diameter.

Axial T2-weighted scans were reviewed as an adjunct to delineate the borders of a tumor and the prostate. They were also used as a reference to precisely identify the borders of transitional zone cancers. Care was taken to avoid placing the ROI onto the extra-prostatic tissues and tumor-free prostatic tissues. To calculate the minimum ADC value of a tumor, the observer placed several circumferential ROIs with a diameter of 10–20 mm onto the tumor. Subsequently, the ROI with the lowest ADC was accepted as the minimum ADC value, as implemented in a previous study.<sup>18</sup>

In addition, the observer drew two separate ROIs for reference. First, an ROI with a minimum diameter of 10 mm onto the contralateral histologically and radiologically tumor-free prostate at the same slice in the same zone. Thereafter, a free-hand ROI covering the whole prostate at the same slice as shown in a previous study.<sup>15</sup> Any area with scarring and inflammation was cautiously excluded; these areas

commonly manifest as areas with low ADC signals while placing the ROI onto the tumor-free prostate. Moreover, the observer avoided positioning the ROI onto the prostate capsule while drawing the free-hand ROI covering the whole prostate. Subsequently, the ROIs were automatically transferred to the cDWI scans. Figures 2 and 3 show an MRI interpretation of patients with peripheral and transitional zone PCa, respectively.

The following parameters were calculated for each index lesion: the mean and minimum tumor ADC ( $ADC_{\text{tumor-mean}}$  and  $ADC_{\text{tumor-min}}$ , respectively); the tumor-free prostatic tissue ADC ( $ADC_{\text{normal}}$ ); the mean tumor ADC ratio calculated by dividing the mean ADC of the tumor by the mean ADC of the normal contralateral tissue ( $ADC_{\text{mean-ratio}}$ ); the minimum tumor ADC ratio calculated by dividing the minimum ADC of the tumor by the mean ADC of the normal contralateral tissue ( $ADC_{\text{min-ratio}}$ ); the mean tumor to whole prostate ADC ratio calculated by dividing the mean ADC of the

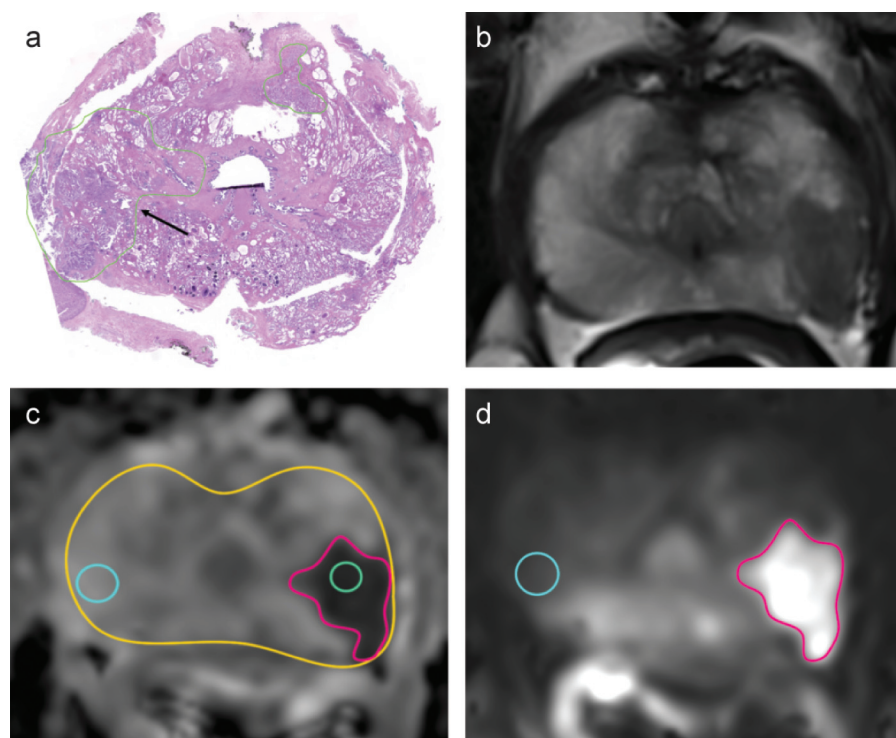


**Figure 2. a-d.** A 59-year-old man with PCa. (a) A highlighted map of the macroscopic whole-mount specimen showing an index lesion with a GS of 4 + 5 in the left peripheral zone at the mid-gland; (b) an axial T2-weighted image at the same level shows an ill-defined hypointense lesion in the left peripheral zone; (c) an axial ADC map of the same patient depicts ROIs for measuring the ADC values of the whole prostate (yellow), tumor-free prostate (blue), minimum (green), and mean tumor ADC (red); (d) an axial calculated DWI of the same patient shows ROIs for measuring the SI of the tumor-free prostate (blue) and mean tumor SI.

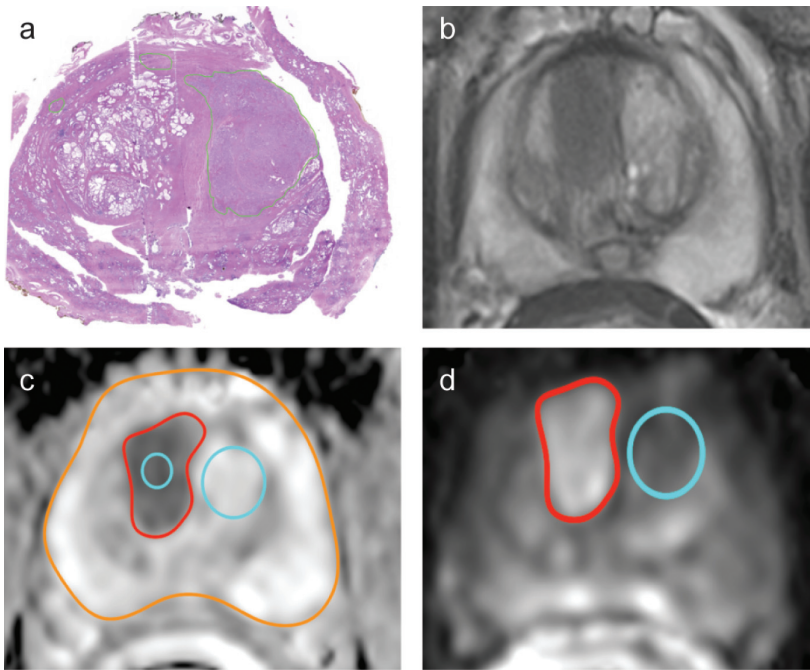


**Figure 3. a-d.** A 64-year-old man with PCa. (a) A highlighted map of the whole-mount specimen shows an index lesion (arrow) with a GS of 4 + 3 in the right transitional zone at the apex; (b) an axial T2-weighted image at the same level shows an ill-defined hypointense lesion; (c) an axial ADC map of the same patient depicts ROIs for measuring the ADC values of the whole prostate (yellow), tumor-free prostate (blue), minimum (green), and mean tumor ADC (red); (d) an axial calculated DWI of the same patient shows ROIs for measuring the SI of the tumor-free prostate (blue) and mean tumor SI.

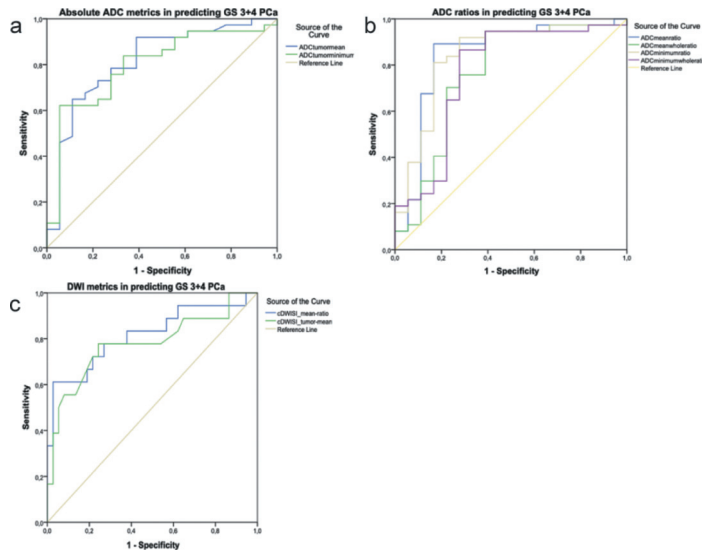


**Figure 4. a-c.** (a) The ROC curves of the absolute ADC ratios in predicting GS 3 + 4 PCa in the ERC data set.  $ADC_{\text{tumor-mean}}$  showed an area under the curve (AUC) of 0.81 ( $P = .001$ ; 95% CI, 0.68-0.94; and SE, 6.59) and  $ADC_{\text{tumor-min}}$  showed an AUC of 0.79 ( $P = .001$ ; 95% CI, 0.67-0.92; and SE, 6.37); (b) the ROC curves of the absolute ADC ratios in predicting GS 3 + 4 PCa in the ERC data set.  $ADC_{\text{mean-ratio}}$  showed an AUC of 0.84 ( $P = .001$ ; 95% CI, 0.71-0.97; and SE, 6.59),  $ADC_{\text{min-ratio}}$  showed an AUC of 0.83 ( $P = .001$ ; 95% CI, 0.70-0.96; and SE, 6.59),  $ADC_{\text{mean-whole-ratio}}$  showed an AUC of 0.76 ( $P = .002$ ; 95% CI, 0.60-0.91; and SE, 7.86), and  $ADC_{\text{min-whole-ratio}}$  showed an AUC of 0.77 ( $P = .002$ ; 95% CI, 0.61-0.91; and SE, 7.61); (c) the ROC curves of the absolute DWI metrics in predicting GS 3 + 4 PCa in the ERC data set.  $cDWI_{\text{SI-tumor-mean}}$  showed an AUC of 0.78 ( $P = .002$ ; 95% CI, 0.63-0.92; and SE, 7.36) and  $DWI_{\text{SI-mean-ratio}}$  showed an AUC of 0.82 ( $P = .001$ ; 95% CI, 0.68-0.95; and SE, 6.85).

tumor by the mean ADC of the whole prostate ( $ADC_{\text{mean-whole-ratio}}$ ); the minimum lesion to whole prostate ADC ratio calculated by dividing the minimum ADC of the tumor by the mean ADC of the whole prostate ( $ADC_{\text{min-whole-ratio}}$ ); the mean lesion SI on cDWI ( $cDWI_{\text{SI-tumor-mean}}$ ); the mean contralateral tumor-free prostatic tissue ( $cDWI_{\text{SI-normal}}$ ); and the mean lesion SI ratio calculated by dividing the mean SI of the tumor by the mean SI of the contralateral normal prostate ( $cDWI_{\text{SI-mean-ratio}}$ ).

### Statistical analysis

Statistical analysis was performed using SPSS software version 22 (IBM). The data were presented with means and standard deviations (SD) for normally distributed continuous variables and medians (interquartile ranges, IQR) for non-normally distributed continuous variables. The categorical data were presented using frequencies and percentages. The performance of the ADC and DWI metrics in assessing PCa aggressiveness was analyzed using receiver operating characteristic (ROC) curves and area under the ROC curves (AUCs). The AUCs were presented with their standard errors (SE) and 95% CI. Youden index was used to determine the best cutoff values on the ROC curves for each metric.<sup>22</sup> The cutoff values determined in the ERC data set were applied to the non-ERC data set, and the sensitivity, specificity, negative predictive value (NPV), positive predictive value (PPV), and accuracy were calculated. The diagnostic accuracies and AUCs of the metrics were compared using Fisher exact test and De Long method, respectively. The diagnostic metrics were presented with their 95% CI. A  $P$  value of less than .05 was considered significant.

Another radiologist with over 2 years of prostate mpMRI experience and the same pathologist jointly evaluated all the patients from the ERC data set to assess the interobserver reliability of the measurements in different sessions. Intraclass correlation coefficients were used to assess interobserver reliability. The ADC and DWI metrics showed good to excellent reliability across two readers.<sup>23</sup> Detailed information regarding the interobserver reliability assessment of the entire ERC data set and of each pair of measurements is given in the supplementary document (Supplementary Table S2.)

Variables	ERC data set (n = 55)	Non-ERC data set (n = 41)
Age (y)*	63.07 ± 7.93 (43-80)	65.10 ± 6.40 (51-78)
Serum PSA level (ng/mL) **	7.1 (4)	6.5 (3)
Prostate volume on mpMRI (cm <sup>3</sup> )**	39.9 (28)	38.6 (27)
PIRADS category (index lesion)		
PIRADS 3	3 (5.45%)	3 (7.32%)
PIRADS 4	30 (54.55%)	21 (51.22%)
PIRADS 5	22 (40%)	17 (41.46%)
Tumor zone (index lesion)		
Peripheral zone	45 (81.82%)	38 (92.70%)
Transition zone	10 (18.18%)	3 (7.30%)
Index lesion diameter on mpMRI (mm)**	11 (8)	14 (10.8)
Tumor foci		
Unifocal	35 (63.63%)	22 (53.70%)
Multifocal	20 (36.36%)	19 (46.30%)
T stage at pathology		
T2	35 (63.63%)	24 (58.54%)
T3a	15 (27.27%)	14 (34.14%)
T3b	5 (9.10%)	3 (7.32%)
N state at pathology		
N0	49 (89.10%)	36 (87.80%)
N1	6 (10.90%)	5 (12.20%)
Final GS (index lesion)		
3 + 4	37 (67.27%)	22 (53.65%)
4 + 3	14 (25.45%)	13 (31.70%)
4 + 4	1 (1.81%)	1 (2.43%)
4 + 5	3 (5.45%)	5 (12.20%)

\*Presented as mean ± SD.  
\*\*Presented as median (IQR).

Variables ADC (× 10 <sup>-3</sup> mm <sup>2</sup> /s)/DW (s/mm <sup>2</sup> )	ERC data set (n = 55)	Non-ERC data set (n = 41)
ADC <sub>tumor-mean</sub>	0.846 ± 0.16	0.794 ± 0.12
ADC <sub>tumor-min</sub>	0.771 ± 0.17	0.743 ± 0.13
ADC <sub>normal</sub>	1.624 ± 2.7	1.504 ± 2.5
ADC <sub>whole</sub>	1.296 ± 2.21	1.421 ± 1.9
ADC <sub>mean-ratio</sub>	0.52 ± 0.08	0.54 ± 0.1
ADC <sub>mean-whole-ratio</sub>	0.65 ± 0.1	0.67 ± 0.14
ADC <sub>min-ratio</sub>	0.48 ± 0.1	0.50 ± 0.10
ADC <sub>min-whole-ratio</sub>	0.6 ± 0.12	0.62 ± 0.13
cDW <sub>SI-tumor-mean</sub>	54.52 ± 23.81	55.60 ± 29.81
cDW <sub>SI-normal-mean</sub>	21.6 ± 11.4	20.32 ± 15.73
cDW <sub>SI-mean-ratio</sub>	3.03 ± 1.92	3.04 ± 1.93

Variables are presented as mean ± SD.

## Results

Overall, 55 men with PCa were enrolled in the ERC data set (age, 63.07 ± 7.93 years; range, 43-80 years), while the non-ERC data set comprised 41 men with PCa (age, 65.1 ± 6.5 years; range, 51-78 years). The detailed clinical and pathological characteristics of the study sample are shown in Table 1. Detailed information regarding the ADC and DWI metrics of the study sample is shown in Table 2.

ADC<sub>mean-ratio</sub> and ADC<sub>min-ratio</sub> yielded the highest AUC, 0.84 ( $P = .001$ ; 95% CI, 0.71-0.97; and SE, 6.59) and 0.83 ( $P = .001$ ; 95% CI, 0.70-0.96; and SE, 6.59), respectively, for differentiating GS 3 + 4 PCa from that with a higher GS, yet the analyses did not reveal any statistically significant differences between ADC and DWI metrics in terms of AUCs ( $P = .214$ ). Figure 4 shows the ROC curves of the ADC and DWI metrics. The best threshold cutoff values of ADC<sub>mean-ratio</sub> (≤0.51) and ADC<sub>min-ratio</sub> (≤0.45) for discriminating GS 3 + 4 PCa from those with higher GS had the highest performance with an accuracy of 87.27% and 85.45%, by predicting 48 and 47 of 55 patients, respectively. However, Fisher exact test yielded no significant difference between the metrics in terms of diagnostic accuracy ( $P = .163$ ). Detailed information regarding the cutoff threshold values for the ADC and DWI metrics and their diagnostic performances are shown in Table 3.

When applied to the non-ERC data set, the ADC<sub>tumor-mean</sub> and ADC<sub>tumor-min</sub> cutoff threshold values of ≤0.818 and ≤0.718 (× 10<sup>-3</sup> mm<sup>2</sup>/s) provided an accuracy of 65.85% (27/41) and 60.97% (25/41), respectively. In the non-ERC data set, ADC<sub>mean-ratio</sub> correctly classified 34 of 41 patients, equating a diagnostic accuracy of 82.92%. However, Fisher exact test yielded no significant difference between the DWI and ADC metrics in terms of diagnostic accuracy in the non-ERC data set ( $P = .561$ ). Detailed information regarding the performances of the cutoff threshold values are shown in Table 4.

## Discussion

The findings of this study showed that the ADC<sub>mean-ratio</sub> yielded the highest diagnostic performance in assessing PCa aggressiveness in the same acquisition settings with good to excellent interobserver reproducibility. However, the performance of different ADC and DWI metrics did not differ in the ERC data set that was

**Table 3.** Diagnostic performance of the ADC and DWI metrics' cutoff thresholds in the ERC data set

ADC ( $\times 10^{-3}$ mm <sup>2</sup> /s)/ DWI (s/ mm <sup>2</sup> )	Cutoff	Performance metrics					Confusion matrix		
		Sen (95% CI)	Spe (95% CI)	NPV (95% CI)	PPV (95% CI)	Acc (95% CI)	Predictions		Ref. test
							Low-grade	High-grade	
ADC <sub>tumor-mean</sub>	≤0.818	77.7 (52.3-93.6)	72.9 (55.8-86.2)	87.1 (73.5-94.2)	58.3 (43.8-71.5)	74.5 (61-85.3)	27	10	Low-grade
							4	14	High-grade
ADC <sub>mean-ratio</sub>	≤0.51	83.3 (58.5-96.4)	89.2 (74.5-96.9)	91.6 (79.5-96.8)	78.9 (59.2-90.6)	87.2 (75.5-94.7)	33	4	Low-grade
							3	15	High-grade
ADC <sub>mean-whole-ratio</sub>	≤0.66	77.7 (52.3-93.6)	64.8 (47.4-79.9)	85.7 (71-93.5)	51.8 (39.4-64.04)	69 (55.1-80.8)	24	13	Low-grade
							4	14	High-grade
ADC <sub>tumor-min</sub>	≤0.718	72.2 (46.5 – 90.3)	75.7 (58.2-88.2)	84.8 (72.2-92.3)	59.1 (43.4-74.1)	74.5 (61-85.3)	28	9	Low-grade
							5	13	High-grade
ADC <sub>min-ratio</sub>	≤0.45	72.2 (46.5 – 90.3)	91.9 (78.1-98.3)	87.1 (76.2-93.5)	81.2 (58.5-93.1)	85.4 (73.3-93.5)	34	3	Low-grade
							5	13	High-grade
ADC <sub>min-whole-ratio</sub>	≤0.59	77.7 (52.3-93.6)	62.1 (44.7-77.5)	85.7 (71-93.5)	50 (38.2-61.8)	67.2 (55.1-80.8)	23	14	Low-grade
							4	14	High-grade
cDWI <sub>SI-tumor-mean</sub>	≥56.6	77.7 (52.3-93.6)	75.7 (58.2-88.2)	87.5 (74.3-94.2)	60.8 (45.5-74.3)	76.3 (62.9-86.7)	28	9	Low-grade
							4	14	High-grade
cDWI <sub>SI-mean-ratio</sub>	≥2.48	77.7 (52.3-93.6)	62.1 (44.7-77.5)	85.7 (71-93.5)	50 (38.2-61.8)	67.2 (55.1-80.8)	27	10	Low-grade
							4	14	High-grade

Metrics are calculated as accepting the GS 3 + 4 PCa as the true negatives (low-grade) and those with higher GS PCa as the true positives (high-grade) accepting the final GS as the reference test.  
Acc, accuracy; NPV, negative predictive value; PPV, positive predictive value; Sen, sensitivity; Spe, specificity.

used for determining the best cutoff values and the non-ERC data set in which the pre-determined cutoff thresholds were assessed for their discriminative ability.

In a previous study, Barrett et al.<sup>8</sup> examined the utility of ADC metrics in characterizing prostate tumors across a diverse set of b-values. The researchers documented that ADC ratios outperformed their absolute counterparts in predicting PCa aggressiveness. Ding et al.<sup>16</sup> and Peng et al.<sup>17</sup> investigated the performance of various ADC metrics in addition to several other T2-weighted imaging and DCE parameters in discriminating low-grade and high-grade PCa in a study sample comprising mpMRI examinations from two different MRI scanner manufacturers. The researchers divided their study sample based on the MRI scanner and then developed several models in each data set to test in the other scanner. In both studies, the 10th percentile ADC yielded the

best performance among other ADC metrics in characterizing PCa aggressiveness, yet the researchers did not investigate the performance of the ADC ratios.<sup>16,17</sup>

A recent potentially related study by Bajgiran et al.<sup>18</sup> investigated various ADC parameters to estimate PCa aggressiveness using a mixed study sample consisting of patients who underwent mpMRI with and without ERC. The performance of the ADC<sub>mean-ratio</sub> surpassed other metrics in discriminating high-grade prostate carcinoma in both patient groups.<sup>18</sup> However, the researchers individually determined different cutoff threshold values for each group; they did not test these cutoff values in an independent validation data set. In this study, we have extended their research by applying cutoff threshold values of ADC and DWI metrics that were determined in the ERC data set to the patients in whom mpMRI was performed without an ERC. In

concordance to the study by Bajgiran et al., the ADC<sub>mean-ratio</sub> consistently yielded the highest diagnostic accuracy in both samples. However, in our study, no significant differences were observed between the performance of different metrics. The sample size of our study was comparably lower than that of Bajgiran et al. (218 vs. 95), and it was further reduced because of separation of the data into two different groups with regard to the use of ERC. Hence, it is likely that the lack of statistical significance between the ADC<sub>mean-ratio</sub> and other metrics might be a consequence of the low sample size.

It should be noted that the benefits of using an ERC are controversial. Some researchers have advocated the use of an ERC at 3T,<sup>24,25</sup> whereas others claimed that there was no increase in image quality with the application of ERC at 3T.<sup>26</sup> Nevertheless, even proponents should consider cost and patient preference; hence, using an ERC

**Table 4.** Independent validation of the cutoff thresholds in the non-ERC data set

ADC ( $\times 10^{-3}$ mm <sup>2</sup> /s)/ DWI (s/ mm <sup>2</sup> )	Performance metrics						Confusion matrix		
	Cutoff	Sen (95% CI)	Spe (95% CI)	NPV (95% CI)	PPV (95% CI)	Acc (95% CI)	Predictions		Ref. test
							Low-grade	High-grade	
ADC <sub>tumor-mean</sub>	≤0.818	68.4 (43.4-87.4)	63.6 (40.6-82.8)	70 (52.8-82.9)	61.9 (46.3-75.2)	65.8 (49.4-79.9)	14	8	Low-grade
							6	13	High-grade
ADC <sub>mean-ratio</sub>	≤0.51	73.7 (48.8-90.8)	90.9 (70.8-98.8)	80 (65-89.5)	87.5 (64.5-96.4)	82.9 (67.9-92.8)	20	2	Low-grade
							5	14	High-grade
ADC <sub>mean-whole-ratio</sub>	≤0.66	73.7 (48.8-90.8)	68.1 (45.1-86.1)	75 (57.2-87.3)	66.6 (50.6-79.6)	70.7 (54.6-83.8)	15	7	Low-grade
							5	14	High-grade
ADC <sub>tumor-min</sub>	≤0.718	57.9 (33.5-79.7)	63.6 (40.6-82.8)	63.6 (48.6-76.3)	57.9 (41.2-72.9)	60.9 (44.5-75.8)	14	8	Low-grade
							8	11	High-grade
ADC <sub>min-ratio</sub>	≤0.45	57.9 (33.5-79.7)	86.9 (65.1-97.9)	70.3 (57.7-80.5)	78.5 (54.5-91.8)	(57.1-85.7)	19	3	Low-grade
							8	11	High-grade
ADC <sub>min-whole-ratio</sub>	≤0.59	57.9 (33.5-79.7)	81.8 (58.2-94.8)	69.2 (56.1-79.8)	73.3 (51.1-87.8)	70.7 (54.6-83.8)	18	4	Low-grade
							8	11	High-grade
cDWI <sub>SI-tumor-mean</sub>	≥56.6	52.6 (28.6-75.5)	81.8 (58.2-94.8)	66.7 (54.5-76.9)	71.4 (48.3-77)	68.2 (51.9-81.9)	18	4	Low-grade
							9	10	High-grade
cDWI <sub>SI-mean-ratio</sub>	≥2.48	63.1 (38.6-83.7)	77.2 (54.6-92.1)	70.9 (56.6-82.1)	70.6 (50.8-84.4)	70.7 (54.4-83.8)	17	5	Low-grade
							7	12	High-grade

Metrics are calculated as accepting the GS 3 + 4 PCa as the true negatives (low-grade) and those with higher GS PCa as the true positives (high-grade) accepting the final GS as the reference test.  
Acc, accuracy; NPV, negative predictive value; PPV, positive predictive value; Sen, sensitivity; Spe, specificity.

might not be suitable for every patient in daily practice. In this context, one might assume that the proportion of prostate mpMRI obtained with an ERC might be decreased in the forthcoming future as the MRI technology continues to advance, and the availability of contemporary 3T scanners steadily increases worldwide. However, currently, quantitative ADC or DWI metrics that could accurately predict PCa aggressiveness across different coil set-ups are still of clinical importance. Additionally, this study's primary aim was not to address the best MRI set-up for assessing PCa aggressiveness; instead, it was to conceive the most stable ADC or DWI metrics across different acquisition settings. Hence, the current discussions on the advantages and disadvantages of using ERC would not invalidate the findings of the present study.

In addition to the low sample size, there are several important limitations to this study. First, the proportion of patients with

transition zone cancer was low, which prevented us from conducting sub-regional analysis. Second, there was an inevitable selection bias since we only enrolled patients who underwent radical prostatectomy. Accordingly, the study cohort did not have any patients managed with active surveillance and included only a few patients with PCa with a very high GS, who rarely undergo surgery. Therefore, the findings of the present study might not be extrapolated to all patients with PCa. Third, the tumor-free ROI was selected based on both mpMRI and whole-mount histopathological images. While the former is readily available in daily practice, it is impossible to use the latter prospectively. Fourth, we employed a slice-based tumor analysis, and several previous studies have proposed that whole lesion analysis is a better and more consistent approach for analyzing PCa.<sup>15</sup> Fifth, we did not investigate the benefits of prostate mpMRI or clinical metrics such as PI-RADS score

and PSA density in assessing PCa aggressiveness or assessing whether ADC and DWI metrics add incremental diagnostic information to these metrics.<sup>27,28</sup> Nevertheless, the main aim of this study was to investigate the most stable ADC or DWI metrics across different acquisition settings rather than assessing their incremental value to such parameters. Finally, in PI-RADS version 2.1, b-values higher than 1000 s/mm<sup>2</sup> were avoided for calculating the ADC map to prevent the diffusion kurtosis effect. However, we incorporated b-values higher than 1000 s/mm<sup>2</sup>, particularly 1400 s/mm<sup>2</sup>, while creating ADC maps, which might negatively influence the metrics' performance.

In conclusion, the ADC<sub>mean-ratio</sub> consistently showed the highest diagnostic accuracy in differentiating GS 3 + 4 PCA from that with a higher GS across different data sets in which prostate mpMRI was performed with and without an ERC, though without any significant difference. Hence,

we believe that the findings of the present study warrant future multi-center studies on a larger scale to precisely reveal the role of the  $ADC_{\text{mean-ratio}}$  as a noninvasive surrogate marker for assessing PCa aggressiveness across different imaging settings.

### Conflict of interest disclosure

The authors declared no conflicts of interest.

### References

- Turkbey B, Rosenkrantz AB, Haider MA, et al. Prostate imaging reporting and data system Version 2.1: 2019 Update of Prostate imaging reporting and data system Version 2. *Eur Urol*. 2019;76(3):340-351. [\[Crossref\]](#)
- Verma S, Rajesh A, Morales H, et al. Assessment of aggressiveness of prostate cancer: Correlation of apparent diffusion coefficient with histologic grade after radical prostatectomy. *AJR*. 2011;196(2):374-381. [\[Crossref\]](#)
- Hambroek T, Somford DM, Huisman HJ, et al. Relationship between apparent diffusion coefficients at 3.0-T MR imaging and Gleason grade in peripheral zone prostate cancer. *Radiology*. 2011;259(2):453-461. [\[Crossref\]](#)
- Vargas HA, Akin O, Franiel T, et al. Diffusion-weighted endorectal MR imaging at 3 T for prostate cancer: Tumor detection and assessment of aggressiveness. *Radiology*. 2011;259(3):775-784. [\[Crossref\]](#)
- Caster JM, Falchhook AD, Hendrix LH, Chen RC. Risk of pathologic upgrading or locally advanced disease in early prostate cancer patients based on biopsy Gleason score and PSA: A population-based study of modern patients. *Int J Radiat Oncol Biol Phys*. 2015;92(2):244. [\[Crossref\]](#)
- Lebovic A, Sfrangeu SA, Feier D, et al. Evaluation of the normal-to-diseased apparent diffusion coefficient ratio as an indicator of prostate cancer aggressiveness. *BMC Med Imaging*. 2014;14:15. [\[Crossref\]](#)
- Boesen L, Chabanova E, Logager V, Balslev I, Thomsen HS. Apparent diffusion coefficient ratio correlates significantly with prostate cancer Gleason score at final pathology. *J Magn Reson Imaging*. 2015;42(2):446-453. [\[Crossref\]](#)
- Barrett T, Priest AN, Lawrence EM, et al. Ratio of tumor to normal prostate tissue apparent diffusion coefficient as a method for quantifying DWI of the prostate. *AJR*. 2015;205(6):585-593. [\[Crossref\]](#)
- Itatani R, Namimoto T, Yoshimura A, et al. Clinical utility of the normalized apparent diffusion coefficient for preoperative evaluation of the aggressiveness of prostate cancer. *Jpn J Radiol*. 2014;32(12):685-691. [\[Crossref\]](#)
- Woo S, Kim SY, Cho JY, Kim SH. Preoperative evaluation of prostate cancer aggressiveness: Using ADC and ADC Ratio in determining Gleason score. *AJR*. 2016;207(1):114-120. [\[Crossref\]](#)
- Rosenkrantz AB, Khalef V, Xu W, Babb JS, Taneja SS, Doshi AM. Does normalisation improve the diagnostic performance of apparent diffusion coefficient values for prostate cancer assessment? A blinded independent-observer evaluation. *Clin Radiol*. 2015;70(9):1032-1037. [\[Crossref\]](#)
- De Cobelli F, Ravelli S, Esposito A, et al. Apparent diffusion coefficient value and ratio as non-invasive potential biomarkers to predict prostate cancer grading: Comparison with prostate biopsy and radical prostatectomy specimen. *AJR*. 2015;204(3):550-557. [\[Crossref\]](#)
- Barbieri S, Brönnimann M, Boxler S, Vermathen P, Thoeny HC. Differentiation of prostate cancer lesions with high and with low Gleason score by diffusion-weighted MRI. *Eur Radiol*. 2017;27(4):1547-1555. [\[Crossref\]](#)
- Waseda Y, Yoshida S, Takahara T, et al. Utility of computed diffusion-weighted MRI for predicting aggressiveness of prostate cancer. *J Magn Reson Imaging*. 2017;46(2):490-496. [\[Crossref\]](#)
- Pierre T, Cornud F, Colléter L, et al. Diffusion-weighted imaging of the prostate: Should we use quantitative metrics to better characterize focal lesions originating in the peripheral zone? *Eur Radiol*. 2018;28(5):2236-2245. [\[Crossref\]](#)
- Hoang Dinh A, Melodelima C, Souchon R, et al. Quantitative analysis of prostate multiparametric MR images for detection of aggressive prostate cancer in the peripheral zone: A multiple imager study. *Radiology*. 2016;280(1):117-127. [\[Crossref\]](#)
- Peng Y, Jiang Y, Antic T, Giger ML, Eggen SE, Oto A. Validation of quantitative analysis of multiparametric prostate MR images for prostate cancer detection and aggressiveness assessment: A cross-imager study. *Radiology*. 2014;271(2):461-471. [\[Crossref\]](#)
- Bajgirani AM, Mirak SA, Sung K, Sisk AE, Reiter RE, Raman SS. Apparent diffusion coefficient (ADC) ratio versus conventional ADC for detecting clinically significant prostate cancer with 3-T MRI. *AJR*. 2019;213(3):W134-W142. [\[Crossref\]](#)
- Epstein JI, Zelefsky MJ, Sjoberg DD, et al. A contemporary prostate cancer grading system: A validated alternative to the Gleason score. *Eur Urol*. 2016;69(3):428-435. [\[Crossref\]](#)
- Samaratunga H, Montironi R, True L, et al. International Society of Urological Pathology (ISUP) Consensus Conference on Handling and Staging of Radical Prostatectomy Specimens. Working group 1: Specimen handling. *Mod Pathol*. 2011;24(1):6-15. [\[Crossref\]](#)
- Ahmed HU. The index lesion and the origin of prostate cancer. *N Engl J Med*. 2009;361(17):1704-1706. [\[Crossref\]](#)
- Altman DG. *Practical Statistics for Medical Research*. New York: Chapman & Hall/CRC Press; 1999.
- Koo TK, Li MY. A guideline of selecting and reporting intraclass correlation coefficients for reliability research (published correction appears in *J Chiropr Med*. 2017 Dec;16(4):346). *J Chiropr Med*. 2016;15(2):155-163. [\[Crossref\]](#)
- Turkbey B, Merino MJ, Gallardo EC, et al. Comparison of endorectal coil and nonendorectal coil T2W and diffusion-weighted MRI at 3 Tesla for localizing prostate cancer: Correlation with whole-mount histopathology. *J Magn Reson Imaging*. 2014;39(6):1443-1448. [\[Crossref\]](#)
- Costa DN, Yuan Q, Xi Y, et al. Comparison of prostate cancer detection at 3-T MRI with and without an endorectal coil: A prospective, paired-patient study. *Urol Oncol*. 2016;34(6):255.e7255.e13. [\[Crossref\]](#)
- Baur AD, Daqqaq T, Wagner M, et al. T2- and diffusion-weighted magnetic resonance imaging at 3T for the detection of prostate cancer with and without endorectal coil: An intraindividual comparison of image quality and diagnostic performance. *Eur J Radiol*. 2016;85(6):1075-1084. [\[Crossref\]](#)
- Faiena I, Salmasi A, Mendhiratta N, et al. PI-RADS Version 2 Category on 3 tesla multiparametric prostate magnetic resonance imaging predicts oncologic outcomes in gleason 3 + 4 prostate cancer on biopsy. *J Urol*. 2019;201(1):91-97. [\[Crossref\]](#)
- Cuocolo R, Stanzione A, Rusconi G, et al. PSA-density does not improve bi-parametric prostate MR detection of prostate cancer in a biopsy naïve patient population. *Eur J Radiol*. 2018;104:64-70. [\[Crossref\]](#)

**Supplemental Table S1.** Prostate mpMRI acquisition parameters

Parameters	Axial TSE T2WI	Sagittal TSE T2WI	Coronal TSE T2WI	Echo planar imaging-DWI	Axial T1W DCE
TR (ms)	5340	5040	3900	4800	4.81
TE (ms)	104	115	117	63	1.74
FOV (mm)	220 × 220	220 × 220	240 × 240	200 × 154	260 × 260
Matrix size	308 × 384	384 × 288	292 × 448	176 × 228	138 × 192
Slice thickness (mm)	3 mm with no interslice gap	3 mm with no interslice gap	3 mm with no interslice gap	3 mm	3 mm with no interslice gap
b-values (s/mm <sup>2</sup> )	-	-	-	50, 500, 1000, 1400	-
Flip angle	160°	144°	160°		15°
Acquisition time (min)	3.2	2.3	3.1	4	2.5

**Supplemental Table S2.** The intraclass correlation coefficient values of the ADC and DWI metrics

Variables ADC (x 10 <sup>-3</sup> mm <sup>2</sup> /s) / DW (s/mm <sup>2</sup> )	Intraclass correlation coefficient values
ADC <sub>tumor-mean</sub>	0.87
ADC <sub>tumor-minimum</sub>	0.93
ADC <sub>mean-ratio</sub>	0.92
ADC <sub>mean-whole-ratio</sub>	0.84
ADC <sub>minimum-ratio</sub>	0.91
ADC <sub>minimum-whole-ratio</sub>	0.87
cDW <sub>SI-tumor-mean</sub>	0.78
cDW <sub>SI-mean-ratio</sub>	0.81

Intraclass correlation coefficient values were calculated with the following parameters: Two-way mixed effects, absolute agreement, and two-raters.

An intraclass correlation coefficient value less than 0.5 is indicative of poor reliability, value between 0.5 and 0.75 indicate moderate reliability, value between 0.75 and 0.9 indicate good reliability, and a value greater than 0.90 indicate excellent reliability.

Additionally, a senior radiologist with over 26 years of prostate MRI interpretation experience explored the inter-observer variability of each single pair of measurements between two observers for all metrics. For any metric that had an absolute difference of an arbitrarily determined cut-off threshold value of > 5% between two observers on a patient basis, the senior radiologist assessed the drawn ROIs the observers to take corrective action, if needed. The senior radiologist identified 8 subjects in whom any of the ADC or DWI metrics showed an absolute difference of more than 5% between two observers. In 7 out of 8 patients, the senior radiologist justified the initial drawings of the first observer. In the remaining case, the senior radiologist corrected the drawn contours, and the ADC and DWI metrics were re-calculated.

The interpretations of the second observer were only used to ensure correctness and the reproducibility of the first observer's measurement. Thereby, they were not taken into account for assessing the performance of the ADC and DWI metrics in discriminating prostate cancers based on the Gleason score.